Scientific Research Publishing

Modern Mechanical Engineering, 2026, 16(3), 33-66
https://www.scirp.org/journal/mme
ISSN Online: 2164-0181
ISSN Print: 2164-0165

Blast Design Optimization in a Fractured Marble Quarry Using Kuz-Ram Modeling and SHOTPlus Simulation: A Case Study from Cameroon (Northern Region)

Aurélie Ngamy Kamwa[1*], Franck Wilfried Nguimatsia Dongmo[1], Francois Ntep[2], Marc Anselme Kamga[3], Nathanael Yaya[1], Sidney Tamasang Asangbeh[1]

[1]Department of Mining Engineering and Mineral Processing, National Advanced School of Mines and Petroleum Industries, University of Maroua, Kaelé, Cameroon
[2]Department of Mining Petroleum and Gas Exploration and Water Resources, National Advanced School of Mines and Petroleum Industries, University of Maroua, Kaelé, Cameroon
[3]Department of Industrial Security, Quality and Environment, National Advanced School of Mines and Petroleum Industries, University of Maroua, Kaelé, Cameroon
Email: *aureliengamy@gmail.com

How to cite this paper: Ngamy Kamwa, A., Nguimatsia Dongmo, F.W., Ntep, F., Kamga, M.A., Yaya, N. and Asangbeh, S.T. (2026) Blast Design Optimization in a Fractured Marble Quarry Using Kuz-Ram Modeling and SHOTPlus Simulation: A Case Study from Cameroon (Northern Region). *Modern Mechanical Engineering*, **16**, 33-66.
https://doi.org/10.4236/mme.2026.163003

Received: March 16, 2026
Accepted: June 22, 2026
Published: June 25, 2026

Abstract

Rock fragmentation efficiency directly influences productivity and operating costs in surface mining. This study presents an integrated approach for optimizing blast design at the Bidzar marble quarry in northern Cameroon, where complex metamorphic geology with dense fracture networks challenges fragmentation control. The methodology combines geological structural mapping, the Kuz-Ram fragmentation model, Langefors-Kihlström empirical design, SHOTPlus Professional simulations, and WipFrag digital image analysis. Four experimental blasts were analyzed, and an optimized design was developed through iterative parameter adjustment in Matlab. Results show that incorporating structural geology parameters, particularly dominant ENE-WSW fracture orientation and discontinuity spacing, significantly improves fragmentation prediction accuracy. The optimized blast configuration (89 mm hole diameter, 3.2 m burden, 3.6 m spacing, 157.3 g/t powder factor) is predicted to reduce oversize fragments (>800 mm) to 3.80%, compared to measured values ranging from 5.40% to 13.24% in the four experimental blasts. The optimized design would achieve a powder factor of 157.3 g/t, which is 27.2% lower than the average of initial blasts (216.1 g/t). SHOTPlus simulations predicted a 95.3% success rate with 4.7% oversize, closely matching Kuz-Ram predictions (3.8% oversize). However, these performance indicators are based on

model predictions; field validation is required to confirm these projected improvements. This study demonstrates that explicitly integrating structural geological data into blast design is essential for fractured rock masses, a factor often overlooked in conventional approaches. The proposed methodological framework offers quarry engineers a practical tool for improving fragmentation efficiency, reducing explosive consumption, and supporting more sustainable mining practices in structurally controlled environments. The approach is applicable to other quarry operations with similar geological conditions.

Keywords

Rock Blasting, Fragmentation Optimization, Kuz-Ram Model, SHOTPlus Simulation, Rock Mass Discontinuities, Image-Based Fragmentation Analysis, Marble Quarry

1. Introduction

Efficient rock fragmentation is a fundamental objective in surface mining and quarrying, as it directly influences the efficiency of downstream operations including loading, hauling, crushing, and grinding [1]-[3]. Fragmentation quality significantly impacts overall productivity, energy consumption, and operational costs. Poorly fragmented rock leads to excessive secondary blasting, increased equipment wear, and higher energy requirements during comminution [4] [5]. Optimizing blasting practices, therefore remains a central challenge in mining engineering.

Blasting efficiency depends on complex interactions between explosive properties, blast geometry, and the mechanical and structural characteristics of the rock mass [6] [7]. Parameters such as burden, spacing, bench height, hole diameter, and charge distribution critically control stress wave propagation and fragmentation patterns [8]-[10]. Over the past decades, numerous empirical and analytical models have been developed to predict blast fragmentation. Among these, the Kuz-Ram model [11] remains the most widely applied, linking explosive characteristics, rock properties, and blast geometry to estimate fragment size distribution [12]. Classical approaches such as the Langefors-Kihlström method provide foundational empirical formulas for bench blasting design [13] [14]. These are increasingly complemented by modern numerical simulations [15] and digital tools including image-based analysis software like WipFrag [16] [17] and specialized simulation environments like SHOTPlus Professional [18] [19].

Despite these technological advances, blast optimization remains particularly challenging in geologically heterogeneous environments where structural discontinuities strongly influence stress wave propagation and fracture development [20] [21]. Rock mass structures such as joints, bedding planes, and faults often exert primary control on blasting efficiency, frequently outweighing explosive

power in determining fragmentation outcomes. The orientation, spacing, and persistence of these discontinuities dictate how explosive energy is distributed and dissipated, resulting in high fragmentation variability even with identical blasting parameters [22] [23]. However, most existing blast optimization studies focus on large-scale open-pit mines in relatively homogeneous rock masses, with limited research addressing structurally controlled marble quarries, particularly in the Central African geological context [24] [25].

The Bidzar quarry, located in northern Cameroon within the Pan-African orogenic belt, exemplifies a structurally complex metamorphic marble deposit. The rock mass comprises alternating marble and schist layers affected by a dense network of fractures and tectonic discontinuities inherited from Pan-African deformation phases [26]-[28]. These structural features, primarily steeply dipping (83˚ SE) N-S striking layers and dominant ENE-WSW fracture sets create a highly anisotropic environment that strongly controls stress wave propagation and fragmentation efficiency. The mechanical contrast between rigid marble (UCS = 75 MPa) and softer schist layers further complicates blast design and fragmentation control.

The novelty of this work lies in developing an integrated blast optimization framework that explicitly accounts for geological structures and rock mass discontinuities in a Pan-African metamorphic quarry environment. By incorporating structural parameters including fracture orientation, discontinuity spacing, and rock mechanical properties into the blast design process, this study aims to improve fragmentation quality while reducing explosive consumption.

The specific objectives of this study are to:

- Characterize the structural geology and rock mass properties of the Bidzar marble quarry;
- Analyze the fragmentation efficiency of current blasting practices through field trials and image-based granulometric analysis;
- Develop an optimized blast design using an integrated approach combining the Kuz-Ram fragmentation model, Langefors-Kihlström empirical design, and iterative parameter adjustment in Matlab;
- Validate the optimized design through SHOTPlus numerical simulations and comparison with WipFrag image analysis results.

By linking empirical fragmentation models, numerical simulation, and image-based analysis with rigorous geological characterization, this study provides a comprehensive methodology for enhancing blast performance in structurally heterogeneous quarry operations. Beyond the Bidzar case study, the proposed approach offers a reproducible and practical solution for improving blasting efficiency in structurally controlled rock masses globally.

2. Geological Setting

The Bidzar quarry is located in northern Cameroon within the North Cameroon Domain of the Central African Pan-African Fold Belt (CAFB). The study area belongs to the Poli Group, a major lithostructural unit composed predominantly of

metasedimentary and metamorphic rocks intruded by Pan-African granitoids [29]-[32] (**Figure 1**).

The Poli Group consists of marbles, schists, metapelites, and associated lithologies that experienced medium, to high-grade metamorphism during the Neoproterozoic Pan-African orogeny (ca. 650-550 Ma). These formations are locally intruded by syn, to post-tectonic granitoids, reflecting a complex polyphase tectonometamorphic evolution related to crustal accretion and continental collision between the Congo Craton and the West African Craton [33]-[36]. The structural architecture of northern Cameroon is thus a central component of the CAFB, characterized by multiple deformation phases that have profoundly influenced the rock mass fabric.

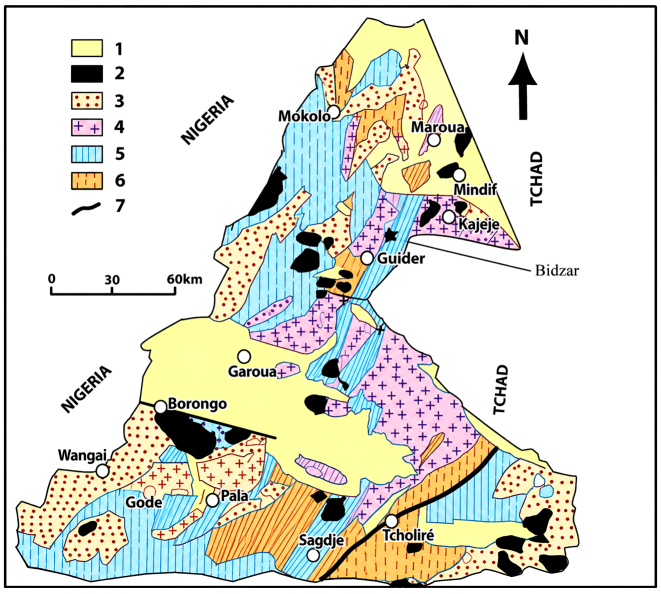

Figure 1. Regional geological map of the Northern Domain of the Central African Pan-African Belt showing the lithostructural units of the Poli Group and the location of the Bidzar quarry study area (modified after [30]). Legend: 1) Phanerozoic formations; 2) Post-tectonic granitoids; 3) Syn- to late-tectonic granitoids; 4) Schist unit; 5) Gneiss unit; (6) Faults.

2.1. Local Geological Structure

The Bidzar quarry, located in the Mayo-Louti Division of northern Cameroon, exploits white, pink, and black marbles for cement production (**Figure 2**). The rock mass exhibits a well-developed metamorphic foliation and a dense network of tectonic discontinuities inherited from Pan-African deformation phases, particularly the D_2 phase [26] [37].

The geological structure is characterized by steeply dipping (83˚ SE) N-S striking marble and schist layers, creating a highly anisotropic environment that strongly controls blasting outcomes (**Figure 3**). Detailed structural mapping reveals three main joint sets (**Figure 4**):

J1 (dominant): ENE-WSW orientation, dipping 75˚ - 85˚;

J2: N-S orientation, dipping 70˚ - 80˚;

J3: E-W orientation, dipping 65˚ - 75˚.

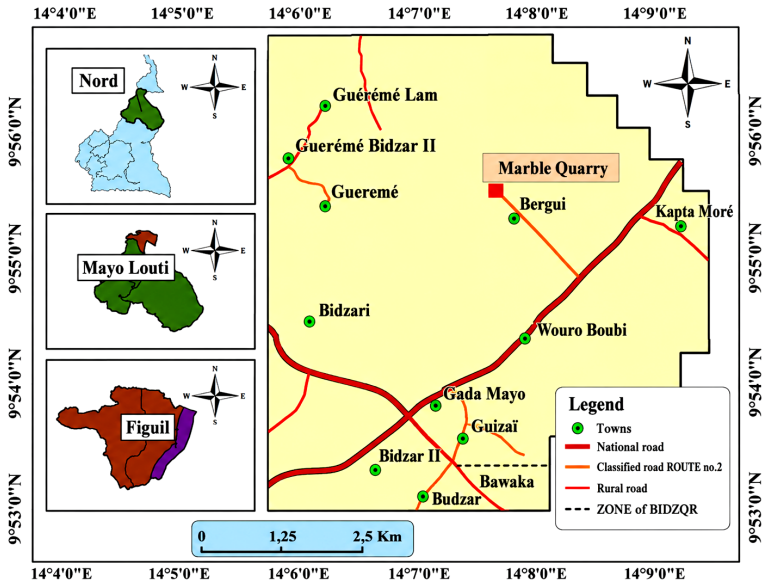

The map was generated by the author using ArcGIS software (Esri, version 10.8). The topographic basemap is derived from SRTM digital elevation data (30 m resolution, NASA/NGA).

Figure 2. Geographic location map of the Bidzar marble quarry in the Mayo-Louti Division, North Region of Cameroon, showing main access routes and surrounding localities.

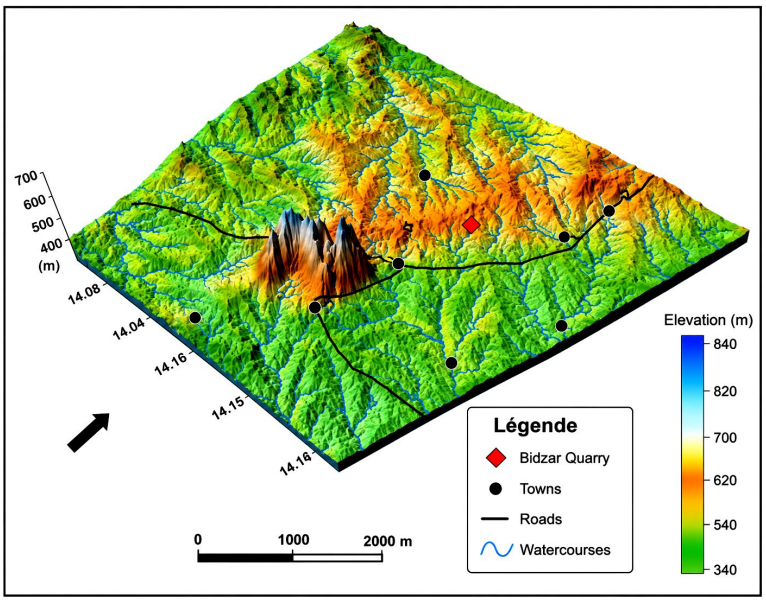

Map source: Generated by author using Surfer software (Golden Software) from SRTM digital elevation data (30 m resolution, NASA/NGA). Quarry boundaries and access roads were mapped using field GPS data collected by author in 2024. Coordinate system: WGS84/UTM zone 33N. Scale bar: 500 m. North arrow indicated.

Figure 3. Topographic map of the Bidzar quarry area showing elevation distribution (contour interval: 10 m) and main geomorphological features.

Figure 4. Field photograph showing the structural arrangement of interbedded marble and schist layers at the Bidzar quarry, with dominant fracture networks (NNE-SSW orientation) controlling rock mass discontinuities and block size distribution.

The ENE-WSW fracture set acts as preferential pathways for stress wave propagation and crack coalescence during blasting, significantly influencing fragmentation efficiency and block detachment [38]. The interaction between these joint sets leads to the formation of prismatic to tabular rock blocks, whose geometry and size directly affect fragmentation outcomes and blast-induced damage.

The lithology comprises alternating sequences of white marble, dolomitic marble, quartzite, and schist/shale units. This lithological contrast creates significant geotechnical heterogeneity: marble layers are rigid and dense (UCS = 75 MPa), while schist layers are softer and more deformable. Previous studies have shown that such heterogeneity complicates fragmentation control, as rigid and deformable materials respond differently to explosive loading [39] [40].

2.2. Rock Mass Properties and Structural Characterization

Field investigations followed ISRM recommended procedures [41]. Scanline surveys were conducted along three orientations (N-S, E-W, and ENE-WSW) with a total cumulative length of **120 m**. A total of **187 discontinuities** were systematically measured for orientation, spacing, persistence, roughness, and aperture. Rock Quality Designation (RQD) was calculated for each 1.5 m scanline segment following Deere [42], yielding an average RQD of 65% (range: 42% - 78%), indicating fair to good rock mass quality with spatial variability correlated to schist content.

For fragmentation analysis using WipFrag, 25 - 30 photographs were taken per

blast pile following standardized protocols (scale reference included in each image, consistent lighting conditions, camera positioned approximately 10 m from the pile). WipFrag 3.3 analyzed each image batch, with manual correction applied to less than 5% of fragment boundaries where automatic detection was incomplete.

The rock mass is affected by a dense network of foliations, joints, and fractures with variable spacing, resulting in a heterogeneous block size distribution [43] [44]. Rock Quality Designation (RQD) index calculated from field measurements according to Deere [42] indicates generally fair to good rock mass quality, with significant spatial variability depending on lithology and fracture density. Lower RQD values are associated with schistose units, whereas higher values correspond to more massive marble layers, consistent with observations in structurally complex metamorphic environments [44] [45].

The physical and mechanical properties of Bidzar marble were measured following standard ASTM and ISRM methods, as summarized in **Table 1**. The marble exhibits a density of 2.77 g/cm^3, uniaxial compressive strength of 75 MPa, Young's modulus of 10.6 GPa, and Poisson's ratio of 0.28. The rock mass factor (A) calculated from Lilly's blastability index [46] is 10.455, a key input parameter for the Kuz-Ram fragmentation model.

From a blasting engineering perspective, these mechanical characteristics play a major role in explosive-rock interaction. The relatively high strength and stiffness of the marble influence stress wave transmission, crack initiation, and fracture propagation around blast holes. When combined with the existing joint network and dominant fracture orientations, these properties directly control fragmentation efficiency, energy consumption, and overall blasting performance. Incorporating these structural parameters into blast design is therefore essential to optimize explosive energy distribution, minimize undesired damage, and improve fragmentation outcomes.

3. Materials and Methods

This study employs a combination of qualitative and quantitative methods to analyze blasting practices at the Bidzar quarry and propose optimized parameters for improved fragmentation. The methodological framework integrates geological site analysis, empirical modeling, numerical simulation, and digital image processing.

3.1. Field Equipment

The following equipment was used for field data collection:

- Digital camera: For photographing blasted rock piles for subsequent granulometric analysis;
- Topcon total station: For precise positioning of drill hole positions and massif configuration assessment;
- Compass and measuring tape: For measuring fracture orientations and dip in the rock mass;

- Moisture meter (digital ohmmeter): For verifying electrical parameters of ignition systems;
- Notebook and field sheets: For recording observations.

3.2. Software Used

Data processing and blasting simulation were performed using:

- WipFrag 3.3: Digital image analysis software for determining granulometric distribution of blasted rock fragments by automatic detection of fragment boundaries and 2D dimension calculation [16].
- Matlab R14: For numerical simulation and systematic parametric optimization of blasting parameters using the Kuz-Ram model [45].
- Orica SHOTPlus Professional: Blasting simulation software for predicting fragmentation based on geotechnical characteristics and explosive charge parameters [46].

3.3. Geotechnical Characterization for Blastability Assessment

Geotechnical properties of the Bidzar quarry rock mass were assessed following standard ASTM and ISRM suggested methods. Detailed methodology for discontinuity mapping, RQD calculation, and mechanical property testing is described in Section 2.3. The complete set of physico-mechanical properties used for blast modeling is presented in Table 1.

Table 1. Physico-mechanical properties of the Bidzar marble rock mass.

Parameter	Value	Unit	Test Standard/Method	Relevance to Blasting
Physical Properties				
Hardness	7.5	Mohs scale	Mohs hardness test	Indicates abrasiveness and drillability
Absolute density	2770	kg/m^3	ASTM C97/ISRM Suggested Methods	Controls explosive-rock impedance matching
Bulk density	2.75	g/cm^3	ASTM C97/ISRM Suggested Methods	Affects weight of material to be blasted
Mechanical Properties				
Uniaxial Compressive Strength (UCS)	75	MPa	ASTM D7012/ISRM UCS	Determines resistance to fragmentation
Indirect tensile strength	8.9	MPa	ASTM D3967/ISRM Brazilian test	Influences crack initiation and propagation
Young's modulus (E)	10.6	GPa	ASTM D7012/ISRM UCS	Controls elastic response and stress wave velocity
Poisson's ratio (ν)	0.28	dimensionless	ASTM D7012/ISRM UCS	Affects rock deformation under dynamic loading
Blastability Index				
Rock mass factor (A)	10.455	dimensionless	Lilly [34] blastability index	Key input parameter for Kuz-Ram fragmentation model

Field investigations followed ISRM recommended procedures [41]. Scanline surveys were conducted along three orientations (N-S, E-W, and ENE-WSW) with a total cumulative length of 120 m. A total of 187 discontinuities were systematically measured for orientation, spacing, persistence, roughness, and aperture. Rock Quality Designation (RQD) was calculated for each 1.5 m scanline segment following Deere [42], yielding an average RQD of 65% (range: 42% - 78%), indicating fair to good rock mass quality with spatial variability correlated to schist content.

For mechanical characterization, 15 block samples were collected from representative locations across the quarry. Uniaxial compressive strength tests (ASTM D7012) were performed on 12 intact specimens (mean = 75 MPa, standard deviation = 4.2 MPa). Indirect tensile strength (Brazilian test, ASTM D3967) was conducted on 10 specimens (mean = 8.9 MPa, standard deviation = 0.7 MPa). Young's modulus was determined from UCS test stress-strain curves (mean = 10.6 GPa, standard deviation = 1.1 GPa).

For fragmentation analysis using WipFrag, 25 - 30 photographs were taken per blast pile following standardized protocols (scale reference included in each image, consistent lighting conditions, camera positioned approximately 10 m from the pile). WipFrag 3.3 analyzed each image batch, with manual correction applied to less than 5% of fragment boundaries where automatic detection was incomplete.

From a blasting engineering perspective, these mechanical characteristics play a major role in explosive-rock interaction. The relatively high strength and stiffness of the marble influence stress wave transmission, crack initiation, and fracture propagation around blast holes. When combined with the existing joint network and dominant fracture orientations, these properties directly control fragmentation efficiency, energy consumption, and overall blasting performance at the quarry.

3.4. Blasting Parameters Modeling (Kuz-Ram and Langefors)

3.4.1. Kuz-Ram Model

The Kuz-Ram model predicts fragment size distribution based on explosive consumption, rock mass characteristics, and blast geometry [11]. The Kuz-Ram model predicts the mean fragment size (X_{50}) using Equation (1):

$$X_{50} = A \times K^{-0.8} \times \left(Q_e\right)^{1/6} \times \left(115/RWS\right)^{19/30} \quad (1)$$

where A is the rock mass factor, K is the powder factor (kg/m^3), Q_e is the mass of explosive per hole (kg), and RWS is the relative weight strength of the explosive compared to ANFO (dimensionless).

For this study, the explosive used was a bulk emulsion with a density of 1.03 g/cm^3 and an RWS of 100 (equivalent to ANFO). This information is critical for accurate fragmentation prediction as the RWS value directly influences the calculated mean fragment size.

The uniformity index (n) was calculated using Cunningham's updated formula [47], which considers drilling accuracy, burden, spacing, and hole geometry.

3.4.2. Langefors-Kihlström Method

The Langefors-Kihlström empirical approach optimizes blast geometric parameters including burden, spacing, and charge concentration based on hole diameter and rock strength [13] [14]. This method remains widely used in Scandinavian blasting practice and provides conservative estimates suitable for fractured rock masses.

The maximum burden ($B_{\max}$) was calculated using the Langefors-Kihlström formula:

$$B_{\max} = (d/33) \times \sqrt{\rho_e \times s / (c \times f \times (E/V))} \quad (2)$$

where:

- d is the hole diameter (mm);
- ρ_e is the explosive density (kg/dm^3);
- s is the weight strength relative to LFB dynamite (dimensionless);
- c is the rock constant (kg/m^3), depending on rock strength and structure;
- f is the degree of fixation factor (1.0 for vertical holes, 1.2 for inclined holes);
- E/V is the energy concentration factor.

For the Bidzar marble, the following parameters were applied:

- Rock constant c = 0.45 kg/m^3 (for medium-hard, fractured rock);
- Fixation factor f = 1.0 (vertical holes);
- Relative weight strength s = 1.0 (emulsion equivalent to LFB).

The practical burden (B) was then derived by applying a correction factor to account for geological structures:

$$B = B_{\max} \times k_{\text{stru}} c_t \quad (3)$$

where $k_{\text{stru}} c_t$ is a structural correction factor (0.85 - 0.95) that accounts for the influence of dominant joint sets (J1: ENE-WSW orientation) on stress wave propagation. This integration of structural geology into the empirical design represents a key innovation of this study.

3.5. Blasting Simulations (SHOTPlus)

Impedance ratio (Z)

The impedance ratio Z characterizes the efficiency of stress wave transmission from the explosive to the rock mass. It is defined as the ratio of explosive mechanical impedance to rock mechanical impedance:

$$Z = \rho_e V_e / \rho_r V_r$$

where:

- ρ_e = explosive density (kg/m^3);
- V_e = explosive detonation velocity (m/s);
- ρ_r = rock density (kg/m^3);
- V_r = P-wave velocity in rock (m/s).

The P-wave velocity in rock can be estimated from the Young's modulus and density using $V_r = \sqrt{E/\rho_r}$ for homogeneous isotropic materials.

For the Bidzar marble (E = 10.6 GPa = 1.06 × 10^{10} Pa, ρ_r = 2770 kg/m^3), $V_r = \sqrt{1.06\times10^{10}/2770} \approx 1956$ m/s.

For the bulk emulsion explosive used in this study (ρ_e = 1030 kg/m^3, V_e = 4500 m/s) and the Bidzar marble (ρ_r = 2770 kg/m^3, V_r = 1956 m/s), the impedance ratio is:

$$Z = 1030\times4500/2770\times1956 \qquad Z = 0.42.$$

According to previous studies, optimal energy transfer from explosive to rock occurs when $Z = 0.4 < Z < 0.7$. The calculated value of 0.42 falls within this optimal range, indicating that the explosive-rock pair is well-matched for efficient fragmentation.

To validate theoretical model results, blast simulations were conducted using Orica SHOTPlus Professional software. This software simulates explosion effects incorporating:

- Rock mass geotechnical properties;
- Blast geometry (burden, spacing, hole diameter, bench height);
- Explosive type and charge distribution;
- Initiation sequence and timing.

Simulations provided predictions of fragment size distribution, oversize percentage, and explosive energy distribution, which were used to iteratively adjust blasting parameters.

3.6. Granulometric Analysis

Images of blasted rock piles were analyzed using WipFrag 3.3 software. The analysis workflow comprised:

- Photograph acquisition under standardized conditions (scale reference included);
- Image calibration and enhancement;
- Automatic fragment boundary detection;
- 2D dimension calculation and statistical analysis;
- Generation of cumulative fragment size distribution curves.

The obtained granulometric distributions were compared with quarry specifications, particularly regarding oversize fragments (>800 mm) and fines (<5 mm).

3.7. Systematic Parametric Optimization Using Matlab

Optimization followed a systematic parametric study approach in Matlab, where key blasting parameters were adjusted incrementally within operational constraints to achieve desired fragmentation outcomes while minimizing explosive consumption.

Parameters varied:

- Burden (B): 2.5 - 3.5 m (0.1 m increments);
- Spacing (S): 3.0 - 4.0 m (0.1 m increments), maintaining S/B ratio between 1.1 and 1.3;
- Stemming length (L_s): 1.5 - 2.0 m (0.1 m increments);

- Subdrilling (J): fixed at 0.7 m (based on quarry practice);
- Explosive charge distribution: adjusted between toe and column charges.

Fixed parameters:

- Hole diameter (d): 89 mm (based on available drilling equipment);
- Bench height (H): 10 m (imposed by quarry operations).

Objective function:

- Minimize proportion of oversize fragments (>800 mm);
- Minimize specific explosive consumption (g/t);
- Maintain uniform fragment size distribution (uniformity index $n > 1.7$).

Constraints:

- Available drilling equipment (89 mm or 102 mm diameter);
- Safety requirements for vibration and flyrock control;
- Geological constraints (fracture orientation and spacing).

For each parameter combination, Matlab calculated:

- Fragment size distribution using the Kuz-Ram model;
- Predicted oversize and fines percentages;
- Powder factor (g/t);
- Cumulative fragmentation curves;
- Uniformity index (n).

The optimal configuration was selected as the parameter set achieving the lowest oversize fraction and powder factor while maintaining acceptable fragmentation uniformity, subsequently validated by SHOTPlus simulations. A total of 1440 parameter combinations were evaluated during the systematic optimization process.

Multi-objective decision criterion for optimal design selection

Given that the three objectives (minimize oversize, minimize powder factor, maximize uniformity) did not always improve simultaneously, a weighted multi-objective utility function U was defined to select the optimal configuration from the 1440 evaluated combinations:

$$U = w_1 \times \left(1 - \text{OversizeOversize}_{\max}\right) + w_2 \times \left(1 - \text{PFPF}_{\max}\right) + w_3 \times \left(n - n_{\min} n_{\max} - n_{\min}\right) + w_4 \times \left(1 - \left|X_{50} - X_{\text{target}}\right| X_{\text{target}}\right)$$

where:

- $\text{Oversize}_{\max}$ = 15% (maximum acceptable oversize fraction);
- $\text{PF}_{\max}$ = 0.6 kg/m^3 (220 g/t, maximum acceptable powder factor);
- $n_{\min}$ = 1.2 (minimum acceptable uniformity index);
- $n_{\max}$ = 2.5 (maximum achievable uniformity index under site conditions);
- X_{target} = 0.35 m (target mean fragment size).

The weights (w_1 = 0.50 for oversize reduction, w_2 = 0.20 for explosive conservation, w_3 = 0.15 for fragmentation uniformity, w_4 = 0.15 for mean size targeting) were assigned based on quarry operational priorities, determined through consultation with CIMENCAM management. The primary concern is minimizing crusher blockages caused by oversize fragments (>800 mm), hence the highest weight (0.50) was assigned to oversize reduction.

The configuration with the highest utility score U that also satisfied all operational constraints (drilling equipment availability: 89 mm diameter only; safety requirements: flyrock control; geological constraints: fracture orientation) was selected as the optimal design. This selection process yielded the 3.2 m × 3.6 m configuration (S/B = 1.125), which achieved the lowest predicted oversize (3.8%) while maintaining PF below 0.45 kg/m^3 (157.3 g/t) and n above 1.7, satisfying all constraints.

4. Results

4.1. Geological Characterization of the Massif

4.1.1. Structural Characteristics

The rock mass at the Bidzar quarry is primarily composed of interbedded marble and schist, exhibiting significant geological heterogeneity. Analysis of fracture orientations using stereographic projection revealed three main joint sets (Figure 5):

- J1 (dominant): ENE-WSW orientation (75˚ - 85˚ dip);
- J2: N-S orientation (70˚ - 80˚ dip);
- J3: E-W orientation (65˚ - 75˚ dip).

The cyclographic traces show a particularly high concentration of fractures in the ENE-WSW direction, indicating that this orientation is dominant in the quarry rock mass. These preferentially oriented fractures, especially J1, facilitate shock wave propagation and contribute to more homogeneous fragmentation in areas where they are concentrated. Conversely, areas with fewer fractures or less favorable orientations tend to produce larger, more irregular fragments.

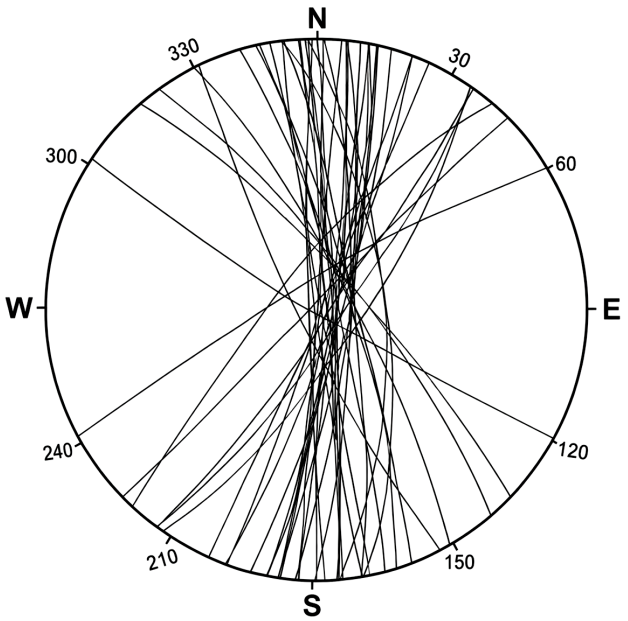

Figure 5. Lower-hemisphere equal-area stereographic projection of discontinuity poles measured in the Bidzar quarry, showing three main joint sets: J1 (ENE-WSW, 75˚ - 85˚), J2 (N-S, 70˚ - 80˚), and J3 (E-W, 65˚ - 75˚). Contours represent 1%, 2%, 4%, and 8% of poles per 1% area.

4.1.2. Geotechnical Characterization of the Rock Mass for Blasting Design

The physical and mechanical properties of Bidzar marble are summarized in Table 1. The rock is characterized by:

- Density: 2.76 g/cm^3 (average);
- Uniaxial compressive strength: 75 MPa;
- Young's modulus: 10.6 GPa;
- Poisson's ratio: 0.28;
- Rock mass factor (A): 10.455.

From a blasting engineering perspective, these characteristics classify the marble as a relatively strong and stiff rock material (Class III, difficult to blast). The relatively high strength and stiffness influence stress wave transmission, crack initiation, and fracture propagation around blast holes. When combined with the existing joint network and dominant fracture orientations, these properties directly control fragmentation efficiency and energy consumption.

4.1.3. Quantitative Rock Mass Characterization for Blastability Inputs

Discontinuity spacing analysis

The three main joint sets identified from stereographic projection (Figure 5) yielded the following spacing statistics:

- J1 (ENE-WSW, dominant): mean spacing = 0.42 m (range: 0.15 - 0.85 m, n = 89 measurements);
- J2 (N-S): mean spacing = 0.68 m (range: 0.30 - 1.20 m, n = 54 measurements);
- J3 (E-W): mean spacing = 0.91 m (range: 0.45 - 1.50 m, n = 44 measurements).

The weighted mean discontinuity spacing across all three sets is 0.59 m, confirming a moderately to highly fractured rock mass where natural discontinuities significantly influence blast-induced fragmentation.

Derivation of Lilly's blastability index (A = 10.455)

Following Lilly (1986), the rock mass factor A was calculated as A = 0.06 × (RMD + JPS + JPA + RDI + HD), where:

- RMD (Rock Mass Description) = 30 (for vertically foliated metamorphic rock with joint spacing less than 1.0 m);
- JPS (Joint Plane Spacing) = 20 (for mean spacing between 0.1 m and 1.0 m);
- JPA (Joint Plane Angle) = 30 (for discontinuity dip between 60˚ and 90˚ relative to the blast face);
- RDI (Rock Density Influence) = 0.025 × ρ_r − 50 = 0.025 × 2750 − 50 = 18.75;
- HD (Hardness) = UCS/5 = 75/5 = 15 (for uniaxial compressive strength between 50 and 100 MPa).

Thus, $A = 0.06 \times (30 + 20 + 30 + 18.75 + 15) = 0.06 \times 174.25 = 10.455$.

Structural correction factor (K_{struct})

The structural correction factor used in Equation (3) was derived from sensitivity analysis of the dominant ENE-WSW fracture set (J1). This factor accounts for the influence of joint orientation on stress wave propagation and was calculated as:

$$A = 0.06 \times (30 + 20 + 30 + 18.75 + 15) = 0.06 \times 174.25 = 10.455.$$

$$K_{\text{struct}} = 1 - \alpha \times (F_{\text{J1}} / F_{\text{max}})$$

where, F_{J1} = measured J1 fracture frequency (fractures/m), F_{max} = maximum J1 fracture frequency (2.4 fractures/m at Bidzar quarry), α = empirical coefficient (0.08 for Bidzar marble).

Where α is an orientation mismatch coefficient ($\alpha = 0$ when blast direction parallels J1 orientation; $\alpha = 0.15$ when misalignment exceeds 30˚). For the optimized design where the blast direction was aligned with the dominant ENE-WSW joint set, K_{struct} was set to 0.95. For zones where J1 orientation is less favorable, values as low as 0.85 were applied, reflecting the reduced fragmentation efficiency when blast direction is misaligned with natural fracture planes by more than 30˚.

4.2. Experimental Blasting Results

Four blast rounds were conducted at the Bidzar quarry with varying parameters. Table 2 summarizes the blast design parameters for each trial.

Table 2. Blasting parameters used during experimental blast rounds at the Bidzar quarry.

Parameters	Blast 1	Blast 2	Blast 3	Blast 4
Blasthole diameter (mm)	102	89	89	89
Impedance ratio (Z)	0.32	0.42	0.42	0.42
Bench height (m)	10	10	10	10
Average hole length (m)	10	10	10	10
Burden (m)	3.5	3.5	3.0	2.5
Spacing (m)	3.5	3.5	3.0	3.0
Stemming length (m)	1.0	1.5	1.75	1.5
Total explosive charge per hole (kg)	49	51	47	42
Rock volume blasted per hole (m^3)	122.5	122.5	90	75
Specific charge (kg/m^3)	0.40	0.42	0.52	0.56
Blast orientation	NNW-SSE & E-W	E-W	NNE-SSW	SSE-NNW

Granulometric analysis of blasted rock was performed using WipFrag 3.3 software (Figure 6).

Key observations (Table 3):

- **Blast 1** (102 mm diameter, PF = 0.40 kg/m^3): Wide fragment size distribution with predominance of larger fragments (12.65% oversize, X_{50} = 373 mm);
- **Blast 2** (89 mm diameter, PF = 0.42 kg/m^3): More homogeneous fragmentation with reduced oversize (11.86%) and mean size (309 mm);
- **Blast 3** (PF = 0.52 kg/m^3): Suboptimal results with increased oversize (13.24%) despite lower mean size (241 mm), suggesting parameters not optimally adapted to local geological conditions;

- **Blast 4** (PF = 0.56 kg/m^3): Best fragmentation performance with lowest oversize (5.40%), mean size of 258 mm, and highest uniformity (n = 2.27).

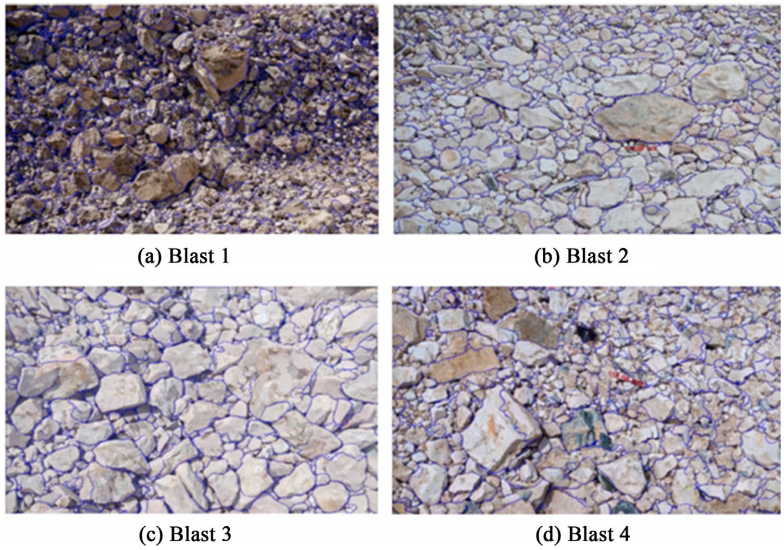

Figure 6. Digital image processing steps for granulometric analysis using WipFrag software: (a) original photograph of blasted rock pile (Blast 4), (b) automatic fragment boundary delineation, (c) color-coded fragment size classification.

Table 3. Presents the fragmentation characteristics for each blast.

Parameters	Blast 1	Blast 2	Blast 3	Blast 4
Specific charge (kg/m^3)	0.40	0.42	0.52	0.56
Powder factor (g/t)	208.2	187.8	261.1	207.4
Oversize percentage (>800 mm) (%)	12.65	11.86	13.24	5.40
Fines percentage (<5 mm) (%)	1.46	2.40	3.76	4.10
Mean fragment size X_{50} (mm)	373.13	309.22	240.82	257.78
Uniformity coefficient (n)	1.72	1.86	2.30	2.27

Figure 7 presents the cumulative fragment size distributions for all four blasts. The curve for Blast 4 exhibits the steepest slope, indicating the most uniform fragmentation with the narrowest size range and lowest proportion of oversize material.

According to company requirements, Blast 4 provides the most satisfactory fragmentation, although it is more demanding in terms of explosive consumption.

4.3. Fragmentation Modeling and Optimization

4.3.1. Kuz-Ram Model Predictions

The Kuz-Ram model was applied to predict fragment size and optimize blasting parameters. Figure 8 shows the predicted fragment size distribution for the optimized blast design, with X_{50} = 420 mm and 3.8% oversize fraction.

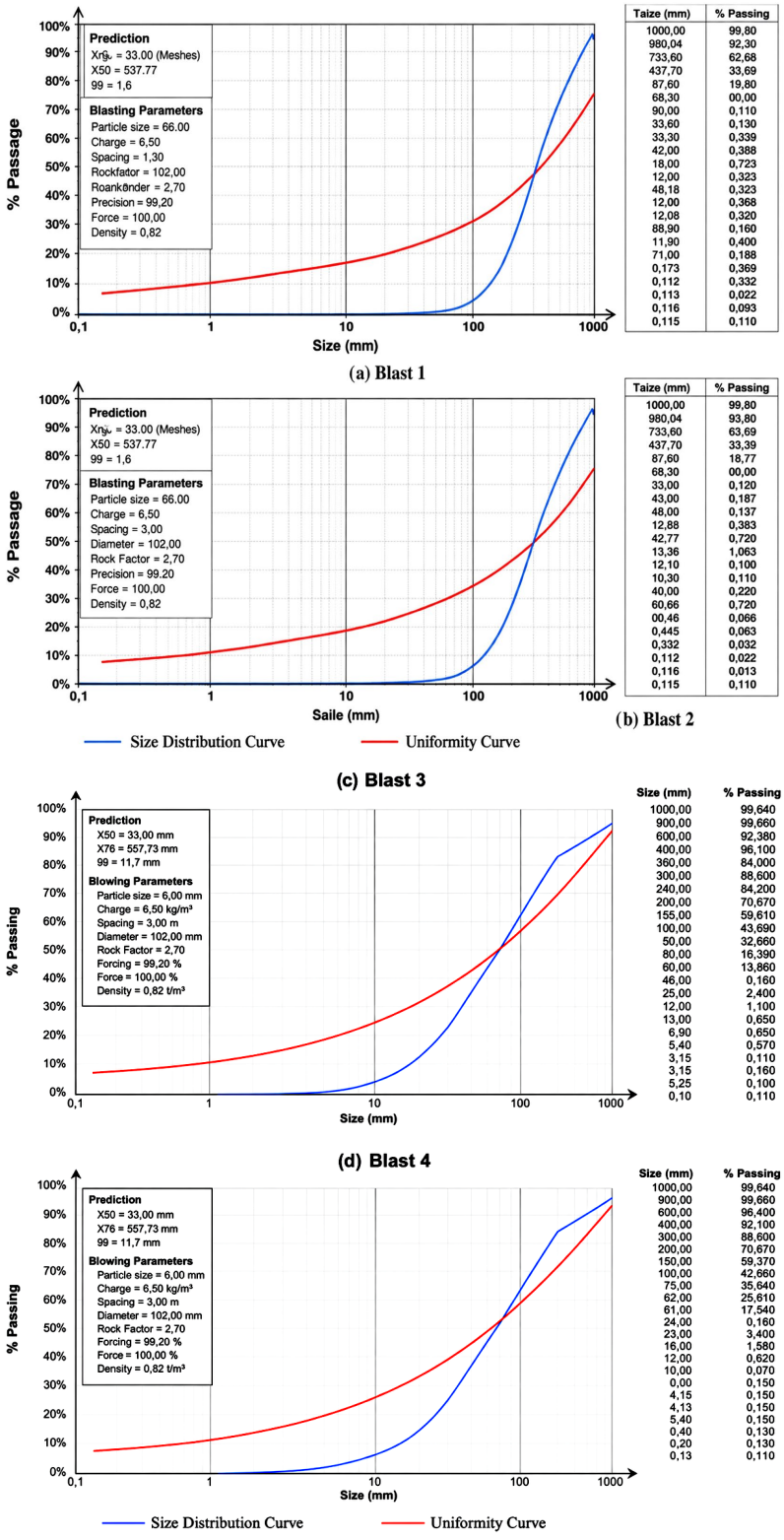

Figure 7. Cumulative fragment size distribution curves obtained from WipFrag image analysis for Blasts 1 - 4 at the Bidzar quarry. The vertical dashed lines indicate the oversize threshold (>800 mm) and the fines threshold (<5 mm). The curve for Blast 4 (red) shows the steepest slope, indicating the most uniform fragmentation with the lowest proportion of oversize fragments.

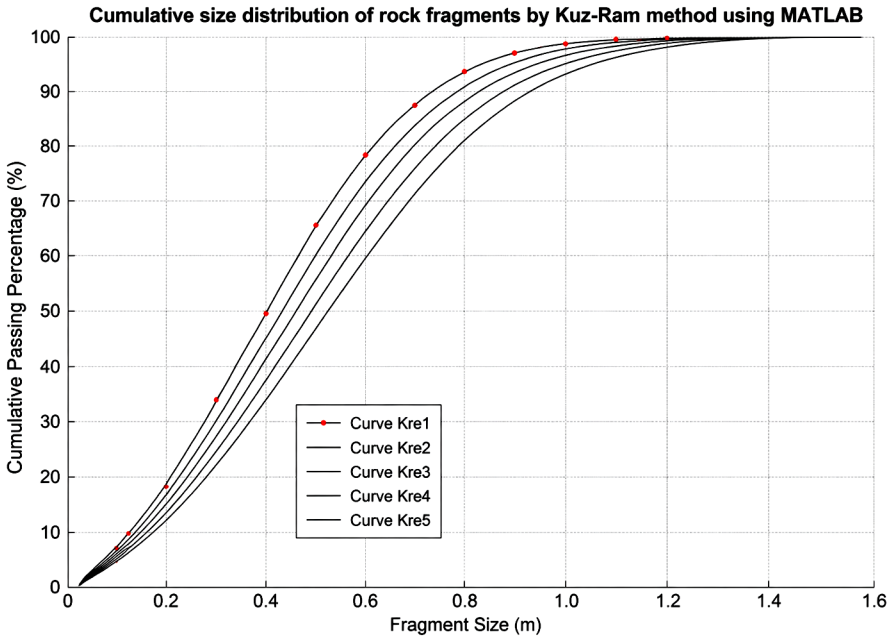

Figure 8. Kuz-Ram model prediction of fragment size distribution for the optimized blast design, showing X_{50} = 420 mm and 3.8% oversize fraction.

Important note: The Kuz-Ram model predictions for the 'Calculated Design' and 'Optimized Design' correspond to a new blast design on a representative section of the quarry. Therefore, the predicted mean fragment sizes (X_{50} of 400 mm and 420 mm) are not directly comparable to the experimental blasts (Blasts 1 - 4), which were conducted in different areas with varying geological conditions and blast parameters. The key performance indicators for comparison are the oversize fraction and the powder factor.

4.3.2. SHOTPlus Simulations

Simulations performed with Orica SHOTPlus Professional software validated the Kuz-Ram model findings. **Figure 9** presents the simulation results for the optimized blast design, showing:

- Blast geometry and explosive charge distribution (**Figure 9(a)**).
- Predicted fragment size distribution with X_{50} = 420 mm and 4.7% oversize (**Figure 9(b)**).
- Energy distribution contours in the rock mass (**Figure 9(c)**).

The close agreement between Kuz-Ram (3.8% oversize) and SHOTPlus (4.7% oversize) predictions validates the robustness of the optimized design through two independent methods.

4.3.3. Optimized Blast Design

Through iterative adjustments in Matlab, the following optimized parameters were identified (**Table 4**):

The overall structure and content of **Table 5** are consistent and well-organized. The units used are appropriate throughout, and the optimized powder factor value

of 157.3 g/t is realistic for the site-specific conditions. The only suggested improvement would be to include a brief explanatory note clarifying the equivalence between grams per tonne (g/t) and kilograms per cubic meter (kg/m^3), as this may help avoid confusion for readers less familiar with this conversion in the context of blasting design.

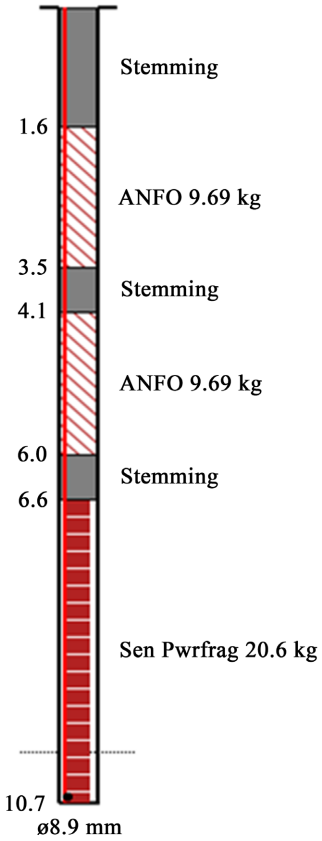

(a)

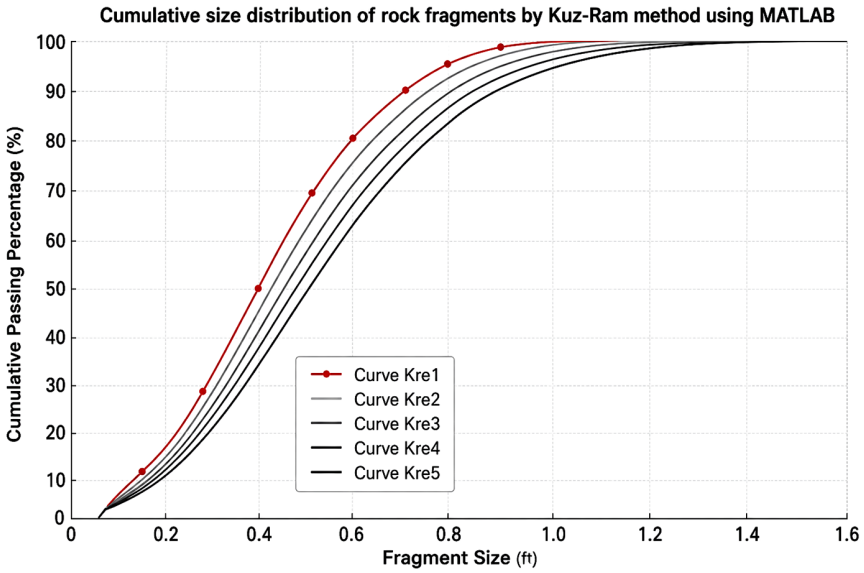

(b)

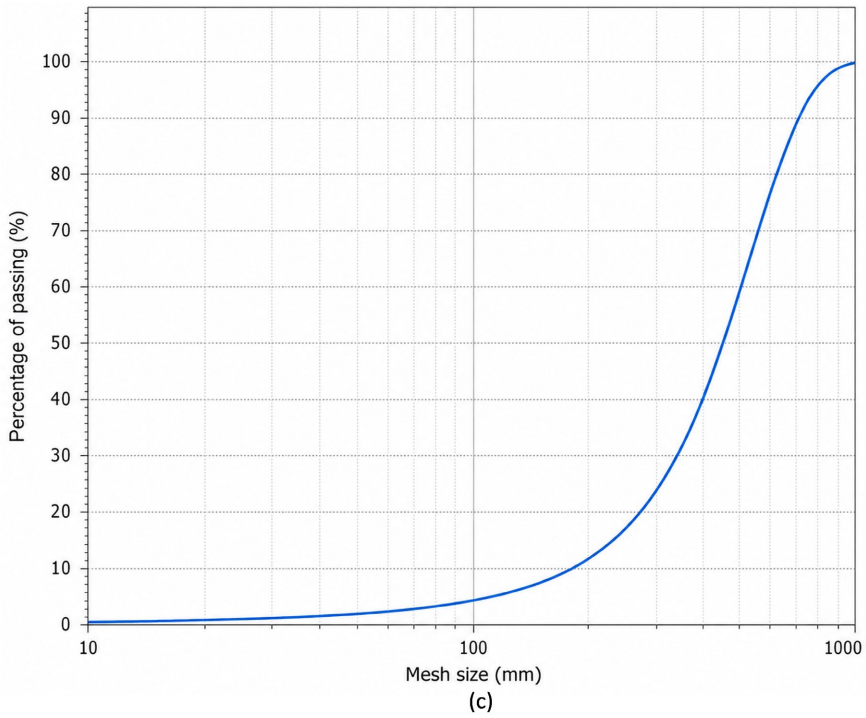

Figure 9. (a) Blast geometry and explosive charge distribution; (b) SHOTPlus Professional simulation results for the optimized blast design (PF = 157.3 g/t): (a) blast geometry and explosive charge distribution, (b) predicted fragment size distribution curve with X_{50} = 420 mm and 4.7% oversize fraction, (c) energy distribution contours in the rock mass.

Table 4. Optimized blast design parameters for the Bidzar quarry.

Category	Parameter	Symbol	Value	Unit
Blast Geometry	Hole diameter	d	89	mm
	Bench height	H	10.0	m
	Hole length	L	10.7	m
	Subdrilling	J	0.7	m
	Burden	B	3.2	m
	Spacing	S	3.6	m
	Drilling angle	α	5	°
	Drilling accuracy	-	0.1	m
Rock Mass Properties	Density	ρ	2.7	g/cm^3
	Uniaxial compressive strength	σc	75	MPa
	Young's modulus	E	10.6	GPa
	Rock mass factor (Lilly, 1986)	A	10.455	-
	Discontinuity spacing	-	<1.0	m
	Discontinuity orientation	-	ENE-WSW	-
	Average dip	δ	83	°

Continued

Explosive Properties	Explosive density	ρ_e	1.03	g/cm^3
	Relative Weight Strength	RWS	100	%
Loading Parameters	Stemming length	L_s	1.6	m
	Foot charge length	L_F	4.1	m
	Column charge length	L_C	5.0	m
	Total charge length	L_t	9.1	m
	Foot charge mass	Q_F	21.3	kg
	Column charge mass	Q_C	25.8	kg
	Total charge per hole	Q_t	47.0	kg
	Specific charge (powder factor)	P_F	157.3	g/t

For reference, a powder factor of 157.3 g/t corresponds to approximately 0.42 kg/m^3 for a rock density of 2.7 t/m^3. Adding this note would enhance clarity and ensure proper interpretation of the specific charge values presented.

Table 5 compares the performance of experimental and designed blasts.

Table 5. Summary of blasting performance indicators for experimental and designed blasts.

Parameter	Blast 1	Blast 2	Blast 3	Blast 4	Calculated Design	Optimized Design	Improvement*
Hole diameter (mm)	102	89	89	89	89	89	-
Powder factor, PF (g/t)	208.2	187.8	261.1	207.4	183.6	157.3	↓ 14.3%[aa] ↓ 27.2%[bb]
Oversize fraction (>800 mm) (%)	12.65	11.86	13.24	5.40	4.50	3.80	↓ 15.6%
Fines fraction (<5 mm) (%)	1.46	2.40	3.76	4.10	0.80	0.90	↑ 12.5%
Mean fragment size, X_{50} (m)	0.373	0.309	0.240	0.257	0.400	0.420	↑ 5.0%
Uniformity index, n	1.72	1.86	2.30	2.27	1.74	1.80	↑ 3.4%

Notes: Blasts 1 - 4 are field-measured results from production blasts conducted at the Bidzar quarry. The "Calculated Design" and "Optimized Design" columns present **predicted results** from Kuz-Ram modeling and SHOTPlus simulations. **The optimized design has not yet been field-tested or validated with production blasts.** Direct numerical comparisons between measured and predicted values are provided for illustrative purposes only to demonstrate the potential improvement suggested by the models. Improvement percentages represent model-based predictions relative to a calculated baseline, not observed field improvements.

The improvement percentages are calculated between the Calculated Design and the Optimized Design, except where indicated otherwise.

- aa: Reduction compared to the "Calculated Design": (183.6 – 157.3)/183.6 = 14.3%.

- bb: Reduction compared to the average of the initial experimental blasts (mean = 216.1 g/t): (216.1 – 157.3)/216.1 = 27.2%.

For reference: A powder factor of 157.3 g/t corresponds to approximately 0.42 kg/m^3 for a rock density of 2.7 t/m^3. This conversion is provided to facilitate comparison with conventional blasting literature.

Although the optimized design shows a slight increase in mean fragment size (X_{50} = 0.42 m) compared to the calculated design (0.40 m), this is accompanied by significant reduction in oversize fragments and improved uniformity. This indicates successful optimization toward a more homogeneous particle size distribution with fewer extreme sizes, which is favorable for downstream processing despite the marginally larger mean size.

5. Discussion

The results obtained from the Bidzar marble quarry demonstrate that blast performance is strongly influenced by the interaction between blast design parameters and rock mass structural characteristics. This discussion interprets these findings in the context of existing literature, highlights the practical implications, and identifies limitations and future research directions.

5.1. Influence of Blast Geometry on Fragmentation Efficiency

Comparison between initial field blasting configurations and the optimized design reveals clear improvements in fragmentation quality and energy efficiency. The reduction in oversize fragments from 12.65% (Blast 1) to 3.80% (Optimized Design) and the more uniform particle size distribution (n increasing from 1.72 to 1.80) indicate that appropriate adjustment of burden, spacing, and charge distribution significantly enhances blasting efficiency in fractured metamorphic rocks. These improvements are consistent with previous studies demonstrating that blast geometry plays a dominant role in controlling explosive energy distribution within the rock mass [4] [8] [10]. Parameters such as burden and spacing directly affect explosive charge confinement conditions and therefore stress wave and detonation gas propagation within blast holes [48] [49]. When these parameters are not properly adapted to local rock conditions, explosive energy may be inefficiently utilized, leading to inadequate fragmentation or excessive boulder formation [12] [50].

The optimized parameters calculated in this study (B = 3.2 m, S = 3.6 m, S/B ratio = 1.125) improved coupling between explosive energy and rock breakage. The 14.3% reduction in powder factor (183.6 → 157.3 g/t) compared to the calculated design, and 27.2% reduction compared to initial blasts average, demonstrates that significant explosive savings can be achieved without compromising and indeed improving fragmentation quality.

5.2. Role of Geological Discontinuities

One of the most significant findings concerns the influence of geological discon-

tinuities on fragmentation efficiency. Structural mapping revealed a dense network of joints and foliations affecting the marble units, with three main joint sets identified (**Figure 5**). The dominant ENE-WSW orientation (J1) acts as natural planes of weakness that significantly influence crack propagation during blasting. Previous research has demonstrated that joint orientation, spacing, and persistence strongly control blast-induced fracture development and fragmentation patterns [22] [23] [43] [44]. In the present case study, fragmentation patterns frequently followed dominant joint orientations, confirming that structural geology plays a decisive role in controlling blast outcomes. Areas with higher fracture density and favorable orientations (ENE-WSW) produced more homogeneous fragmentation, while areas with fewer fractures or less favorable orientations generated larger, more irregular fragments.

The 15.6% reduction in oversize fragments achieved by the optimized design (from 4.50% to 3.80%) can be partially attributed to aligning the blast geometry with the dominant ENE-WSW joint set (J1). By orienting the blast direction parallel to this preferential fracture orientation and adjusting the burden and spacing to match the natural discontinuity spacing (<1.0 m), the design enhanced the utilization of these natural planes of weakness. This alignment facilitated more efficient stress wave propagation and crack coalescence along pre-existing fractures, resulting in improved fragmentation with lower explosive energy requirements. Quantitatively, the optimized design achieved this oversize reduction while simultaneously decreasing powder factor by 14.3%, demonstrating that proper alignment with geological structures can yield dual benefits: better fragmentation quality and reduced energy consumption.

The integration of structural geological information into the blast design process therefore represents a critical step toward improving blasting efficiency in structurally heterogeneous deposits. Similar integrated approaches combining geomechanical characterization and blast modeling have been recommended in recent mining research [6] [7]. By incorporating geological observations into the modeling workflow, this study achieved more realistic fragmentation predictions and reduced uncertainty associated with purely empirical design methods.

5.3. Validation through Multiple Methods

The combined use of image-based fragmentation analysis (WipFrag), empirical modeling (Kuz-Ram), and numerical simulation (SHOTPlus) provided robust validation of the optimized blast design.

Image-based analysis: WipFrag results clearly showed progressive improvement from Blast 1 to Blast 4, with Blast 4 achieving the most favorable fragment size distribution (**Figure 7**). Image-based techniques are increasingly used in mining operations because they provide rapid, objective, and reproducible particle size distribution measurements [16] [17] [51]. The clear reduction in coarse fragments and more favorable distribution of intermediate particle sizes observed in this study are particularly important for quarry operations where crusher perfor-

mance directly depends on initial blast fragmentation [52] [53].

Numerical simulation: SHOTPlus simulations validated the optimized configuration, with predicted oversize of 4.7% closely matching the Kuz-Ram prediction of 3.8% (**Figure 8** and **Figure 9**). Simulation tools allow engineers to visualize explosive energy distribution and test multiple blast configurations before field implementation [19] [21] [46]. This predictive capability significantly reduces operational risks and supports development of more efficient blast designs. The close agreement between independent prediction methods strengthens confidence in the optimized design.

Limitation: Predicted versus measured results

It is important to explicitly acknowledge a limitation of this study. The optimized blast design (3.2 m burden, 3.6 m spacing, 157.3 g/t powder factor) was developed through iterative parametric optimization in Matlab and validated through two independent prediction methods (Kuz-Ram and SHOTPlus). However, this optimized design has not yet been implemented and measured in the field. Therefore, comparisons between the predicted performance of the optimized design (3.8% oversize) and the measured performance of experimental blasts (5.40% - 13.24% oversize) should be interpreted as model-based projections of potential improvement rather than directly observed gains under identical conditions. Direct numerical comparisons (e.g., "15.6% reduction in oversize") are presented as illustrative examples of what the models suggest could be achieved, not as verified field results.

The four experimental blasts (Blasts 1 - 4) were conducted in different areas of the quarry with varying geological conditions and blast parameters. The optimized design was modeled for a representative section of the quarry, but field validation remains necessary to confirm whether the predicted improvements materialize under actual operating conditions. Future work should prioritize field implementation of the optimized design with subsequent WipFrag analysis to validate these predictions.

5.4. Interpretation of Mean Fragment Size Increase

It is worth noting that the optimized design resulted in a slight increase in mean fragment size (X_{50}) from 0.40 m to 0.42 m (+5%), which might appear contradictory to the objective of improving fragmentation. However, this increase should be interpreted in the context of overall fragmentation optimization strategy.

The primary goal was to reduce the proportion of oversize fragments (>800 mm), which decreased significantly from 4.50% to 3.80% (−15.6%). Simultaneously, the uniformity index (n) improved from 1.74 to 1.80, indicating a narrower and more homogeneous fragment size distribution around the mean. In practice, a more uniform distribution with fewer extreme sizes (both oversize and fines) is often more desirable for downstream operations such as crushing and grinding, even if the mean fragment size increases slightly.

This trade-off between mean size, oversize reduction, and uniformity is typical

in blast optimization, where the goal is not simply to minimize X_{50}, but to achieve a particle size distribution that maximizes overall mine-to-mill efficiency [4] [19]. The optimized design successfully balanced these competing objectives, delivering better fragmentation quality with lower explosive consumption.

5.5. Economic Implications

The following is a scenario analysis based on assumed production rates and estimated costs. All values are for illustration only and do not represent guaranteed savings.

The reduction in explosive consumption achieved through blast optimization has direct economic benefits. The optimized design resulted in a decrease of approximately 27.2% in explosive usage compared to the average of initial blasts (216.1 → 157.3 g/t), while simultaneously improving fragmentation quality. Similar economic benefits have been reported in several mining operations where improved fragmentation reduces drilling, blasting, and crushing costs across the mine-to-mill chain [1] [4] [5] [48].

Assumptions for the scenario analysis:

The following assumptions were used in this analysis:

- Annual quarry production: 1,000,000 tonnes per year (based on CIMENCAM-Figuil internal production reports, 2023);
- Bulk emulsion explosive price: Based on industry benchmarks, the estimated price of bulk emulsion in Central Africa is approximately $1200 - $1500 per tonne delivered (personal communication with supplier, 2024);
- Exchange rate: 1 USD = 600 FCFA (BEAC reference rate, 2024);
- Secondary blasting cost: $2 - $5 per tonne of oversize material (estimated range based on industry standards; source: [44]);
- Crusher productivity gain: 3% - 5% increase for each 10% reduction in oversize (estimated based on [52]; requires site-specific validation);
- Equipment wear reduction: Estimated at $15,000 - $25,000 per year (industry average for similar operations; see [1]).

Calculated potential savings:

Under the assumed production rate of 1 million tonnes per year, the predicted reduction in powder factor from 216.1 g/t (average of initial blasts) to 157.3 g/t (optimized design) represents a decrease of 58.8 g/t, equivalent to approximately 58.8 tonnes of explosive per year. At the estimated price range for bulk emulsion in Central Africa ($1200 - $1500 per tonne), this translates to estimated annual explosive savings of $70,000 - $88,000 (approximately 44 - 53 million FCFA).

Additional potential benefits, if the predicted fragmentation improvements materialize, could include:

- **Reduced secondary blasting:** From 5.40% measured oversize in Blast 4 (the best-performing experimental blast) to 3.80% predicted oversize would reduce oversize material by approximately 16,000 tonnes per year. At an estimated secondary breakage cost of $2 - $5 per tonne, this could save $32,000 - $80,000

annually (19 - 48 million FCFA).

- **Improved crusher throughput:** A 15.6% reduction in oversize fragments could increase crusher productivity by an estimated 5% - 8%, potentially generating energy and maintenance savings of $25,000 - $40,000 per year (15 - 25 million FCFA).
- **Reduced equipment wear:** More uniform fragmentation could reduce wear on excavator buckets, crusher jaws, and conveyor belts, estimated at $15,000 - $25,000 per year (10 - 15 million FCFA).
- **Total estimated potential annual benefit:** $190,000 - $315,000 (approximately 115 - 190 million FCFA) under the assumed production scenario.

Important caveats:

The following limitations apply to this economic analysis:

1) All savings are estimates based on predicted fragmentation improvements that have not yet been field-validated

2) The production rate of 1,000,000 tonnes per year is assumed for scenario calculation; actual quarry production may vary.

3) Explosive prices are estimates based on regional benchmarks and personal communication with supplier; actual prices depend on negotiated contracts, volume discounts, and transportation costs.

4) Secondary blasting and crusher productivity estimates are drawn from industry literature; site-specific values may differ considerably.

5) Exchange rates fluctuate; FCFA values are calculated at the 2024 reference rate.

The authors strongly recommend conducting a detailed cost-benefit analysis using site-specific operational data and, crucially, field validation of the optimized blast design before making any investment or operational decisions based on these estimates.

These economic benefits also have environmental implications, as reduced explosive consumption lowers nitrogen oxide and carbon dioxide emissions associated with explosive manufacture and detonation, contributing to more sustainable mining practices. In the Cameroonian context, where the mining sector is expanding, such improvements align with national objectives for industrial competitiveness and sustainable resource development.

5.6. Limitations and Future Research

Despite these promising results, several limitations should be acknowledged:

Model limitations: The Kuz-Ram model, although widely used, remains an empirical approach that simplifies the complex physics of rock blasting. The model does not fully represent dynamic interactions between stress waves, detonation gases, and rock mass discontinuities [20] [21]. Discrepancies between predicted and observed fragmentation may occur in highly heterogeneous rock masses.

Geological variability: This research was conducted in a single marble quarry characterized by specific geological conditions within the Pan-African belt of Central Africa. While the methodological framework is broadly applicable, additional

case studies in different geological environments would help validate its general applicability.

Future research directions:

Advanced numerical modeling: Integration of discrete element modeling (DEM) or hybrid continuum-discontinuum simulations could improve fragmentation prediction accuracy by better representing dynamic fracture propagation through discontinuities [20] [21].

Multi-site validation: Comparative studies involving various lithologies (limestone, granite, sandstone), structural conditions, and explosive types would further improve understanding of blast optimization strategies.

Mine-to-mill integration: Future work should track the impact of improved fragmentation on downstream crushing and grinding efficiency to quantify full economic benefits [52] [53].

Real-time monitoring: Integration of drone-based image acquisition and real-time fragmentation analysis could enable adaptive blast design based on immediate feedback.

Environmental impact assessment: Detailed quantification of reduced emissions from lower explosive consumption would strengthen the sustainability case for optimized blasting.

5.7. Practical Recommendations

Based on this study, the following practical recommendations are proposed for blast optimization in fractured rock masses:

1) Conduct detailed structural mapping before blast design to identify dominant joint sets and orientations.

2) Integrate geological parameters into fragmentation models rather than relying on generic rock mass classifications.

3) Use multiple prediction methods (empirical models + numerical simulation) to validate blast designs.

4) Implement image-based fragmentation analysis for routine monitoring and feedback.

5) Consider the trade-off between mean fragment size, oversize reduction, and powder factor in optimization objectives.

6) For quarries in the Central African region, prioritize the use of locally-relevant economic metrics (FCFA) when presenting cost-benefit analyses to stakeholders.

6. Conclusion

This study demonstrates that blast design optimization integrating geological structural data significantly improves fragmentation efficiency in fractured metamorphic quarries. Through the combined use of the Kuz-Ram model, Langefors-Kihlström design principles, SHOTPlus simulations, and WipFrag image analysis at the Bidzar marble quarry in northern Cameroon, several key findings emerge.

The optimized blast configuration is predicted to reduce oversize fragments (>800 mm) to 3.80%, compared to measured values ranging from 5.40% to 13.24% in the four experimental blasts analyzed. This represents a potential improvement in fragmentation uniformity (n increasing from 1.72 to 1.80 in model predictions). The optimized design would also achieve a powder factor of 157.3 g/t, which is 27.2% lower than the average of initial blasts (216.1 g/t). Under an assumed production scenario of 1 million tonnes per year, this would translate to estimated annual explosive savings of approximately 58.8 tonnes, with corresponding economic benefits estimated at 190,000 - 190,000 - 315,000 (115 - 190 million FCFA). However, these performance indicators are based on Kuz-Ram model predictions and SHOTPlus simulations; field validation is required to confirm these projected improvements.

A critical finding is the essential role of geological structure in fragmentation control. The dominant ENE-WSW fracture orientation (J1) and discontinuity spacing were shown to directly influence stress wave propagation and crack coalescence. The potential reduction in oversize fragments to 3.80% predicted by the optimized design can be partially attributed to aligning blast geometry with these natural planes of weakness, demonstrating that structural geology must be incorporated into blast design for heterogeneous rock masses.

The close agreement between Kuz-Ram predictions (3.8% oversize) and SHOTPlus simulations (4.7% oversize) confirms the reliability of the optimized design from a modeling perspective, while WipFrag image analysis provided objective quantification of fragmentation improvements from the four experimental blasts. The slight increase in mean fragment size (X_{50} from 0.40 m to 0.42 m) alongside reduced oversize and improved uniformity illustrates that blast optimization should focus on the entire particle size distribution rather than minimizing X_{50} alone.

Based on these findings, systematic structural mapping should be conducted before blast design, geological parameters must be integrated into fragmentation models, multiple prediction methods should be used for validation, and routine image-based fragmentation analysis should be implemented for monitoring and feedback.

Study limitation: The authors acknowledge that the optimized blast design presented in this study has not yet been field-tested. All performance claims for the optimized design (3.8% oversize, 157.3 g/t powder factor, 95.3% SHOTPlus success rate) are based exclusively on Kuz-Ram model predictions and SHOTPlus simulations, not on field measurements. The four experimental blasts (Blasts 1 - 4) were conducted in different areas of the quarry with varying geological conditions and blast parameters; they serve as baseline references for comparison, not as direct comparators to the optimized design. Field implementation of the optimized design and subsequent fragmentation analysis using WipFrag are necessary to validate these predictions under actual production conditions at the Bidzar quarry.

This integrated approach provides a robust and transferable framework for improving the efficiency, safety, and sustainability of blasting operations in fractured rock masses worldwide, with direct applications in quarries and open-pit mines facing similar structurally controlled challenges.

Acknowledgements

The authors thank the management and technical staff of the Bidzar quarry for their support and access to the site during field investigations. Special thanks go to **Pr. Dikwa** for his valuable assistance with the SHOTPlus simulations and to the University of Maroua for providing the laboratory facilities.

Conflicts of Interest

The authors declare no conflicts of interest regarding the publication of this paper.

References

[1] Sanchidrián, J.A., Segarra, P. and López, L.M. (2007) Energy Components in Rock Blasting. *International Journal of Rock Mechanics and Mining Sciences*, **44**, 130-147. https://doi.org/10.1016/j.ijrmms.2006.05.002

[2] Zhang, Z.X. (2016) Rock Fracture and Blasting: Theory and Applications. Butterworth-Heinemann.

[3] Hustrulid, W. (1999) Blasting Principles for Open Pit Mining. A.A. Balkema.

[4] Workman, L. and Eloranta, J. (2003) Cost Effective Blast Design through the Use of Bulk Emulsions. *Proceedings of the* 29*th Annual Conference on Explosives and Blasting Technique*, Nashville, 2-5 February 2003, 1-12.

[5] Yang, Q., Gao, Q., Jia, Y., Zhou, H., Gao, X., Jiang, W., *et al*. (2025) Application of Simulation Methods and Image Processing Techniques in Rock Blasting and Fragmentation Optimization. *Applied Sciences*, **15**, Article 3365. https://doi.org/10.3390/app15063365

[6] Himanshu, V.K., Mishra, A.K., Roy, M.P. and Singh, P.K. (2023) Rock-Explosive Interaction during Underground Blasting. In: Himanshu, V.K., Mishra, A.K., Roy, M.P. and Singh, P.K., Eds., *Blasting Technology for Underground Hard Rock Mining*, Springer, 25-48. https://doi.org/10.1007/978-981-99-2645-9_3

[7] Mitchell, T.R., Wang, Z., Araos, M., Leonardi, C.R., Gefken, P.R. and Onederra, I.A. (2022) Experimental and Numerical Investigation into the Fracture Patterns Induced by Blast-Loading under Unconfined and Confined Conditions. *Rock Mechanics and Rock Engineering*, **56**, 2433-2455. https://doi.org/10.1007/s00603-022-03195-x

[8] Salmi, E.F. and Sellers, E.J. (2021) A Review of the Methods to Incorporate the Geological and Geotechnical Characteristics of Rock Masses in Blastability Assessments for Selective Blast Design. *Engineering Geology*, **281**, Article ID: 105970. https://doi.org/10.1016/j.enggeo.2020.105970

[9] Akyildiz, O. and Hudaverdi, T. (2020) ANFIS Modelling for Blast Fragmentation and Blast-Induced Vibrations Considering Stiffness Ratio. *Arabian Journal of Geosciences*, **13**, Article No. 1162. https://doi.org/10.1007/s12517-020-06189-7

[10] Cunningham, C.V.B. (1983) The Kuz-Ram Model for Prediction of Fragmentation from Blasting. *Proceedings of the* 1s*t International Symposium on Rock Fragmentation by Blasting*, Luleå, 23-26 August 1983, 439-454.

[11] Agyei, G. and Asssua, P. (2022) Predicting Fragmentation Distribution of Rock Blasting at Eshiem Pit of Aliko Resources Limited, Ghana. *Nigerian Journal of Technology*, **41**, 651-661. https://doi.org/10.4314/njt.v41i4.3

[12] Langefors, U. and Kihlström, B. (1963) The Modern Technique of Rock Blasting. Wiley.

[13] Bar, L., Sarr, D., A. Sall, O. and Gueye, E.H.M. (2025) Blasting Analysis on the Basalt of Diack (Senegal) Using the Langefors-Kihlstrom Theory. *International Journal of Research and Review*, **12**, 143-152. https://doi.org/10.52403/ijrr.20250418

[14] Zhang, Z.X. (2025) Overview of Rock Blasting Theory and Its Engineering Applications. *Proceedings of the* 14*th International Symposium on Rock Fragmentation by Blasting*, Antalya, 7-10 April 2025, 7-10.

[15] Franklin, J.A. and Maerz, N.H. (1988) Photographic Measurements of Jointing and Fragmentation. *International Symposium on Field Measurements in Geomechanics*, **2**, 227-237.

[16] Batouche, T., Tabet, A., Zerzour, O., Hadji, R., Benyoucef, A.A., Moueri, A., *et al*. (2025) Optimizing Rock Fragmentation in Open Pit Mining: Blasting Plan Refinement Using WipFrag and Kuz-Ram Method. *Geomatics*, *Landmanagement and Landscape*, No. 4, 77-89. https://doi.org/10.15576/gll/193744

[17] Degold, F. (2025) Advanced Blast Planning with New Technologies for Conventional Tunneling. In: Johansson, F., Ansell, A., Johansson, D., Funehag, J. and Norrman, J., Eds., *Tunnelling into a Sustainable Future—Methods and Technologies*, CRC Press, 2084-2090. https://doi.org/10.1201/9781003559047-266

[18] Shields, L., Silva, J., Calnan, J., Maldonado, E. and Agioutantis, Z. (2024) Integrating Underground Blast Fragmentation Modeling for Sustainable Mine-To-Mill Optimization: A Focus on Blast Fragmentation and Energy Efficiency in Comminution Circuits. *Rock Mechanics and Rock Engineering*, **58**, 4497-4508. https://doi.org/10.1007/s00603-024-04118-8

[19] Leon, F., Rojas, L., Peña, A., Moraga, P., Robles, P., Gana, B., *et al*. (2025) Mathematical Modelling and Optimization Methods in Geomechanically Informed Blast Design: A Systematic Literature Review. *Mathematics*, **13**, Article 2456. https://doi.org/10.3390/math13152456

[20] Lin, Q., Cheng, Q., Li, K., Xie, Y. and Wang, Y. (2020) Contributions of Rock Mass Structure to the Emplacement of Fragmenting Rockfalls and Rockslides: Insights from Laboratory Experiments. *Journal of Geophysical Research*: *Solid Earth*, **125**, e2019JB019296. https://doi.org/10.1029/2019jb019296

[21] Deressa, G.W., Choudhary, B.S. and Jilo, N.Z. (2025) Advanced Bench Design and Technical Challenges in Open Pit Mining: A Comprehensive Review of Stability and Productivity. *Arabian Journal of Geosciences*, **18**, Article No. 28. https://doi.org/10.1007/s12517-024-12157-2

[22] Deressa, G.W., Choudhary, B.S. and Jilo, N.Z. (2025) Optimizing Blast Design and Bench Geometry for Stability and Productivity in Open Pit Limestone Mines Using Experimental and Numerical Approaches. *Scientific Reports*, **15**, Article No. 5796. https://doi.org/10.1038/s41598-025-90242-6

[23] Wouatong, A., Kenmoe, O., Ngapgue, F., Katte, V. and Kamgang, V. (2017) A Geological and Physico—Mechanical Characterization of Marble of the Bidzar Quarry North-Cameroon. *British Journal of Applied Science & Technology*, **19**, 1-11. https://doi.org/10.9734/bjast/2017/30421

[24] Mbanga, A.F., Moussango Ibohn, A.P., Sep Nlomngan, J.P., Mahamat, A., Wassouo Wadjou, J., Fodoué, Y., *et al*. (2023) Structures and Petrography of the Neoprotero-

zoic Rey Bouba Greenstone Belt in the Northern Cameroon: Implications for Deformational Characterization. *Arabian Journal of Geosciences*, **16**, Article No. 67. https://doi.org/10.1007/s12517-022-11115-0

[25] Djifack, J.E., Kanouo, N.S., Sabiha, A.B., Hamadou, T. and Basua, E.A.A. (2024) Marbles and Meta-Schists from Bidzar (North Region of Cameroon): Characteristics and the Use of Meta-Schists as Additives in Experimenting Blended Cements Production. *Engineering Research Express*, **6**, Article ID: 045004. https://doi.org/10.1088/2631-8695/ad8723

[26] Askaripour, M., Saeidi, A., Mercier-Langevin, P. and Rouleau, A. (2022) A Review of Relationship between Texture Characteristic and Mechanical Properties of Rock. *Geotechnics*, **2**, 262-296. https://doi.org/10.3390/geotechnics2010012

[27] Xie, H., Pei, J., Zuo, J. and Zhang, R. (2011) Investigation of Mechanical Properties of Fractured Marbles by Uniaxial Compression Tests. *Journal of Rock Mechanics and Geotechnical Engineering*, **3**, 302-313. https://doi.org/10.3724/sp.j.1235.2011.00302

[28] Toteu, S.F., Van Schmus, W.R., Penaye, J. and Michard, A. (2001) New U-Pb and SM-ND Data from North-Central Cameroon and Its Bearing on the Pre-Pan African History of Central Africa. *Precambrian Research*, **108**, 45-73. https://doi.org/10.1016/s0301-9268(00)00149-2

[29] Toteu, S.F., Penaye, J. and Djomani, Y.P. (2004) Geodynamic Evolution of the Pan-African Belt in Central Africa with Special Reference to Cameroon. *Canadian Journal of Earth Sciences*, **41**, 73-85. https://doi.org/10.1139/e03-079

[30] Ipan, A.S., Bondjè, L.M.N.B., Betsi, T.B., Fotze, Q.M.A., Nlomgan, J.P.S. and Bitom, D.L. (2022) Litho-Structural Mapping of Bipindi-Lolodorf Area, South Cameroon: Mining Implication. *Arabian Journal of Geosciences*, **15**, Article No. 617. https://doi.org/10.1007/s12517-022-09814-9

[31] Azefack Mbounou, R.L., Ganno, S., Ngnotue, T., Tanko Njiosseu, E.L., Fossi, D.H., Ngassam Mbianya, G., *et al*. (2023) Structural and Kinematic Analysis of the Nkondjock Shear Zone, Central Cameroon: Implications on the Geodynamic Evolution of the Central African Fold Belt. *Arabian Journal of Geosciences*, **16**, Article No. 240. https://doi.org/10.1007/s12517-023-11336-x

[32] Ngako, V., Affaton, P. and Njonfang, E. (2008) Pan-African Tectonics in Northwestern Cameroon: Implication for the History of Western Gondwana. *Gondwana Research*, **14**, 509-522. https://doi.org/10.1016/j.gr.2008.02.002

[33] Njonfang, E., Ngako, V., Moreau, C., Affaton, P. and Diot, H. (2008) Restraining Bends in High Temperature Shear Zones: The "central Cameroon Shear Zone", Central Africa. *Journal of African Earth Sciences*, **52**, 9-20. https://doi.org/10.1016/j.jafrearsci.2008.03.002

[34] Kankeu, B. (2010) Polyphase Deformation and Evidence for Transpressive Tectonics in the Kimbi Area, Northwestern Cameroon Pan-African Fold Belt. Ph.D. Thesis, University of Yaounde 1.

[35] Ngako, V., Emmanuel, N., Julien, B., Jean Marcel, A.E., Mero, Y., Augustin Patrice, M.I., Sylvestre, N., Yaya, F. and Zénon, I. (2023) Analogue Upright Folds in the Sao Francisco Congo Craton Deformed Margin, Central African Fold Belt (CAFB): Inferences to the Western Gondwana Tectonic Evolution. *Journal of Tectonics*, **7**, 63-80.

[36] Ntouala, R.F.D., Ndjankoum, B.E., Ndome-Priso, E., Binel, M.T.N., Onana, V.L. and Ekodeck, G.E. (2024) Mineralogical, Geochemical, and Physico-Mechanical Features of Bidzar (North Cameroon) Termite Mound Materials and Its Suitability in Producing Fired Bricks with Marble Powder Additive. *Journal of the Cameroon Academy of*

Sciences, **20**, 39-54. https://doi.org/10.4314/jcas.v20i1.3

[37] Gül, M. and Uslular, G. (2016) Geomorphological Features and Weathering of the Southern Submassif of the Menderes Massif (SW Turkey). *Arabian Journal of Geosciences*, **9**, Article No. 682. https://doi.org/10.1007/s12517-016-2715-0

[38] Ulusay, R. (2014) The Present and Future of Rock Testing: Highlighting the ISRM Suggested Methods. In: Ulusay, R., Ed., *The ISRM Suggested Methods for Rock Characterization, Testing and Monitoring*: 2007-2014, Springer, 1-22. https://doi.org/10.1007/978-3-319-07713-0_1

[39] Deere, D.U. (1964) Technical Description of Rock Cores for Engineering Purposes. *Rock Mechanics and Engineering Geology*, **1**, 16-22.

[40] Hoek, E. and Brown, E.T. (1997) Practical Estimates of Rock Mass Strength. *International Journal of Rock Mechanics and Mining Sciences*, **34**, 1165-1186. https://doi.org/10.1016/s1365-1609(97)80069-x

[41] Palmstrom, A. (2005) Measurements of and Correlations between Block Size and Rock Quality Designation (RQD). *Tunnelling and Underground Space Technology*, **20**, 362-377. https://doi.org/10.1016/j.tust.2005.01.005

[42] Hoek, E., Carter, T.G. and Diederichs, M.S. (2013) Quantification of the Geological Strength Index Chart. *International Journal of Rock Mechanics and Mining Sciences*, **56**, 113-122.

[43] Lilly, P.A. (1986) An Empirical Method of Assessing Rock Mass Blastability. *Large Open Pit Mining Conference*, *Australasian Institute of Mining and Metallurgy*, Newman, October 1986, 89-92.

[44] Trivedi, R., Singh, T.N. and Raina, A.K. (2016) Simultaneous Prediction of Blast-Induced Flyrock and Fragmentation in Opencast Limestone Mines Using Back Propagation Neural Network. *International Journal of Mining and Mineral Engineering*, **7**, 237. https://doi.org/10.1504/ijmme.2016.078350

[45] Bascur, O.A. (2024) The Engineering Science of Mineral Processing: A Fundamental and Practical Approach. CRC Press.

[46] Remli, S., Benselhoub, A. and Rouaiguia, I. (2019) Optimization of Blasting Parametrs in Open Cast Quarries of El Hassa-Bouira (Northern Algeria). *GeoScience Engineering*, **65**, 53-62. https://doi.org/10.35180/gse-2019-0006

[47] Cunningham, C.V.B. (1987) Fragmentation Estimations and the Kuz-Ram Model—Four Years On. *Proceedings of the* 2*nd International Symposium on Rock Fragmentation by Blasting*, Keystone, 23 August 1987, 475-487.

[48] Sanchidrián, J.A., Segarra, P. and López, L.M. (2005) A Practical Procedure for the Measurement of Fragmentation by Blasting by Image Analysis. *Rock Mechanics and Rock Engineering*, **39**, 359-382. https://doi.org/10.1007/s00603-005-0073-4

[49] Lawal, A.I. (2021) A New Modification to the Kuz-Ram Model Using the Fragment Size Predicted by Image Analysis. *International Journal of Rock Mechanics and Mining Sciences*, **138**, Article ID: 104595. https://doi.org/10.1016/j.ijrmms.2020.104595

[50] Agyei, G. and Owusu-Tweneboah, M. (2019) A Comparative Analysis of Rock Fragmentation Using Blast Prediction Results. *Ghana Mining Journal*, **19**, 49-58. https://doi.org/10.4314/gm.v19i1.6

[51] Nanda, S. and Pal, B.K. (2020) Analysis of Blast Fragmentation Using WipFrag. *International Journal of Innovative Science and Research Technology*, **5**, 1561-1566. https://doi.org/10.38124/ijisrt20jun1086

[52] Navarro Torres, V.F., Ferreira, F.V., de Carvalho, V.A., Veras, E. and Sitônio, F.F. (2024) Application of Blast-Pile Image Analysis in a Mine-To-Crusher Model to Min-

imize Overall Costs in a Large-Scale Open-Pit Mine in Brazil. *Mining*, **4**, 983-993. https://doi.org/10.3390/mining4040055

[53] Saadoun, A., Boukarm, R., Fredj, M., Menacer, K., Boudjellal, D., Hafsaoui, A., *et al*. (2024) Optimal Blast Design Considering the Effects of Geometric Blasting Parameters on Rock Fragmentation: A Case Study. *ARPHA Proceedings*, **7**, 136-146. https://doi.org/10.3897/ap.7.e0136

Nomenclature

Symbol	Description	Unit
ρ	Bulk density	g/cm^3
σc	Uniaxial compressive strength	MPa
E	Young's modulus	GPa
ν	Poisson's ratio	-
A	Rock mass factor	-
B	Burden	m
S	Spacing	m
H	Bench height	m
d	Hole diameter	mm
PF	Powder factor (specific charge)	g/t
X_{50}	Mean fragment size	mm
n	Uniformity index	-
RQD	Rock Quality Designation	%

Abbreviations and Acronyms

Abbreviation/Acronym	Definition
ANFO	Ammonium Nitrate Fuel Oil
ASTM	American Society for Testing and Materials
CAFB	Central African Pan-African Fold Belt
DEM	Discrete Element Modeling
ISRM	International Society for Rock Mechanics
J1, J2, J3	Joint Sets 1, 2, and 3 (dominant fracture orientations)
RQD	Rock Quality Designation
RWS	Relative Weight Strength
UCS	Uniaxial Compressive Strength